Rhodium thiolate hydroformylation complexes tethered to delamellated γ-zirconium phosphate

Sergio Rojas, Sonia Murcia-Mascarós,* Pilar Terreros and José Luis García Fierro

Instituto de Catálisis y Petroleoquímica, CSIC, Cantoblanco, 28049, Madrid, Spain.
E-mail: smascaros@icp.csic.es; Fax: + 34 91 585 4760

Received (in Montpellier, France) 17th May 2001, Accepted 30th July 2001
First published as an Advance Article on the web 19th October 2001

Rhodium thiolate complexes intercalated in crystalline γ-zirconium phosphate or tethered to SiO_2-modified γ-zirconium phosphate have been synthesised. It was observed that the addition of a solution of organic silicates to a colloidal suspension of γ-zirconium phosphate yielded amorphous substrates, which displayed very high specific areas (160–650 $m^2\ g^{-1}$). Incorporation of a mercaptocarbonyl rhodium complex resulted in a highly selective and active catalyst precursor for the hydroformylation of 1-heptene in the liquid phase. Elemental analysis and photoelectron spectroscopy of the fresh and used samples revealed that some metal leaching occurs during the reaction, this being mainly confined to the outer layers of the solid particles. This observation, together with the high selectivity towards linear aldehydes, makes SiO_2-modified γ-zirconium phosphate a good support candidate for immobilised Rh catalysts. Spectroscopic data obtained from the crystalline precursor and also from the amorphous catalyst showed that the interaction between the rhodium complex and the acid support was achieved *via* hydrogen bonds, forming NH groups.

The hydroformylation of olefins in the presence of homogeneous catalysts has been applied commercially for the production of aldehydes from olefins for many years.[1] Most efforts have concentrated on the use of rhodium complexes as catalysts because they often exhibit substantially higher activity than other transition metal catalysts when working under mild reaction conditions.[2–5] However, the benefits of the homogeneous process are in many instances overshadowed by the inherent difficulty involved in separating the catalyst from the reaction products and the deactivation that arises due to irreversible structural changes. In order to overcome these problems, much work has been devoted to tethering homogeneous complex catalysts to solid carriers in order to exploit the advantage of high activity and selectivity of soluble complexes with easy catalyst recovery.[6] Many heterogenisation strategies have been employed for this purpose. They include attaching complexes to Merrifield resins[7,8] and dendrimers,[9] using polymerisable ligands to form the backbone of the support,[10] incorporating catalysts into a siloxane matrix,[11] trapping catalysts inside the micropores of a zeolite,[12] encapsulating catalysts in an organic[13] or inorganic[14] polymer, using catalyst–substrate solubility differences in biphasic catalysis,[15,16] and using soluble polymer supports.[17] Among these, inorganic oxides, SiO_2 [18–20] and Al_2O_3 [21] are often preferred because of their rigid structure and high stability in different reaction conditions. Silica is doubtless the most widely used support since transition metal complexes can be easily tethered to its surface through alkoxy or chlorosilane functional groups of the ligand that react with surface hydroxyl groups on silica. Recently, some examples of Rh anchored on zirconium and titanium phosphates have been described.[22,23]

Our aim in the present work was to prepare a new class of inorganic carriers consisting of zirconium phosphates that can tether rhodium complexes[24,25] useful for hydroformylation reactions. γ-Zirconium phosphate (γ-ZrP) is a layered acidic material in which the protons can be exchanged with metal ions or polyoxocations.[26] It has recently been reported that γ-ZrP can swell in acetone–water mixtures with no layer structural changes.[27] This procedure was used in the present contribution to prepare colloidal dispersions of γ-ZrP, which can flocculate in acid media in the presence of some soluble silica precursors to yield highly dispersed amorphous γ-ZrP/SiO_2 supports.[28] These materials were used to tether rhodium thiolate complexes, which were subsequently tested in 1-heptene hydroformylation under mild reaction conditions. Although rhodium complexes are active for the hydroformylation of alkenes, only a few attempts have been made to conduct the reaction over its thiolate complexes tethered to silica[29–31] or to phosphinated cross-linked polystyrene.[32]

Experimental

Chemicals

Zirconium oxide chloride-8-hydrate (Riedel-de-Haen p.a.), tetraethylsilicate (Aldrich), tetrapropylammonium hydroxide (Aldrich), 4,6-dimethyl-2-mercaptopyrimidine (HSpym), 1-heptene (Aldrich, gas-chomatography purity), 1,5-cyclooctadiene (COD, Merck, 99% purity) and $RhCl_3 \cdot xH_2O$ (Johnson Matthey Chemicals) were used. All other chemicals (Panreac), of the highest commercially available purity were used as received. High purity CO (99.995 vol%) and H_2 (99.995 vol%) gases were provided by Air Liquide.

Synthesis of supports and complexes

Crystalline support. The preparation of γ-ZrP has been described previously.[33] It basically consists of mixing a 2 M $NH_4H_2PO_4$ aqueous solution with a solution containing HF and $ZrOCl_2 \cdot 8H_2O$. The resulting solution was maintained at 353 K for 24 h and the mono-ammonium form of the γ-ZrP was obtained. Then, this solid was contacted with a 1 M HCl solution to obtain the acid form: $ZrPO_4H_2PO_4 \cdot 2H_2O$.

 DOI: 10.1039/b104339k

Amorphous support. The amorphous support was prepared following a previously described procedure.[27] Basically, 1 g of γ-ZrP was suspended in 50 mL of a 1 : 1 water–acetone mixture and kept under reflux. Then, a solution of tetrapropylammonium hydroxide and tetraethylsilicate, containing 15% SiO_2, was added. Subsequently, 1 M acetic acid solution was added to the final mixture at room temperature. The gel thus obtained was dried at 353 K and finally calcined in air at 873 K for 2 h.[28] Hereafter, the support is referred to as 20-ZPS (27 mL of silicate solution was used) and 40-ZPS (10 mL of silicate solution was used).

Synthesis of complexes. All preparations of rhodium complexes were carried out using standard Schlenk techniques under an inert atmosphere. [Rh(Spym)$(CO)_2$], (RhSCO) was prepared according to our method.[34] Scheme 1 shows the routes for the synthesis of the RhSCO complex. [Rh(μ-Cl)-$(CO)_2]_2$ was prepared from a suspension of [Rh(μ-Cl)$(COD)]_2$ (prepared following a previously described method[35]) in hexane, by bubbling CO at 273 K for 30 min. An insoluble red–orange solid was filtered off and dried. The FTIR spectra in ether showed bands centred at 2110(m), 2092(s), 2080(w), 2037(vs) and 2006(w) cm^{-1}, as previously reported.[36] Its powder X-ray diffraction pattern matched the previously reported crystalline structure (ICDD-PDF n° 83-529).[37]

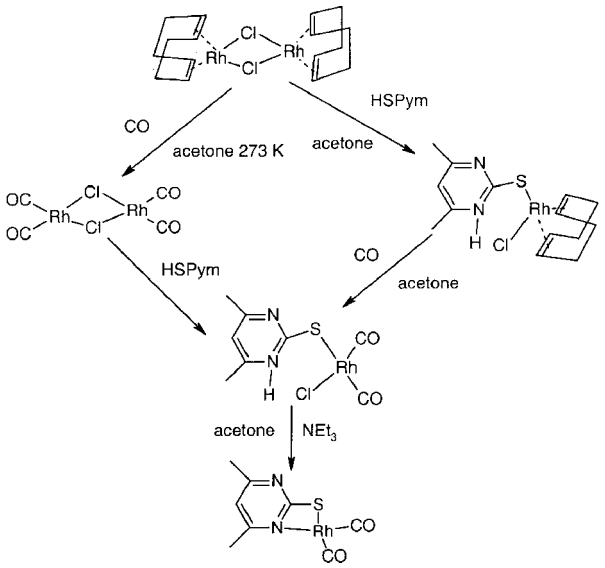

Scheme 1 Synthetic pathway for RhSCO and intermediate complexes.

Tethering and exchange procedures

Crystalline pathway. The solid S1 was prepared by intercalation of the thiopyrimidine ligand (HSpym). In particular, 0.251 g of γ-ZrP was suspended in 50 mL of an acetone–water (3 : 1) mixture containing 0.223 g of HSpym. The suspension was stirred vigorously at 338 K for 11 days, after which the solid was separated by filtration and washed with acetone (Scheme 2, top). Then, 0.120 g of the solid S1 was added to 50 mL of an acetone–water solution containing 0.020 g of the [Rh(μ-Cl)$(CO)_2]_2$ complex and the same procedure was followed, yielding the solid S2. The solid S3 was prepared from 0.028 g of RhSCO complex and 0.246 g of crystalline γ-ZrP by a procedure similar to those described above.

Amorphous pathway. For the preparation of the tethered catalysts, 0.502 g of the 20-ZPS support was suspended in 40 mL of an acetone–water (3 : 1) mixture containing 0.010 g of RhSCO while 0.422 g of the 40-ZPS support was suspended in 80 mL of an acetone–water (3 : 1) mixture containing 0.021 g of RhSCO. The suspension was stirred vigorously at 338 K for 11 days, after which the solid was separated by filtration, washed with acetone and dried at 353 K. Solids RhS20 and RhS40, respectively, were obtained (Scheme 2, bottom). The supernatant solution was analysed in order to determine its Rh content. The synthesis procedures, labelling, rhodium content, BET specific area and mesoporous volume of all the aforementioned solids are shown in Table 1.

Characterisation

The samples were characterised by X-ray diffractometry using a computerised Seifert 3000XRD diffractometer equipped with a bent graphite monochromator and an automatic slit using Cu-Kα radiation ($\lambda = 0.154\,06$ nm).

Elemental chemical analysis of the zirconium phosphate tethered catalysts as well as of the mother liquor from the

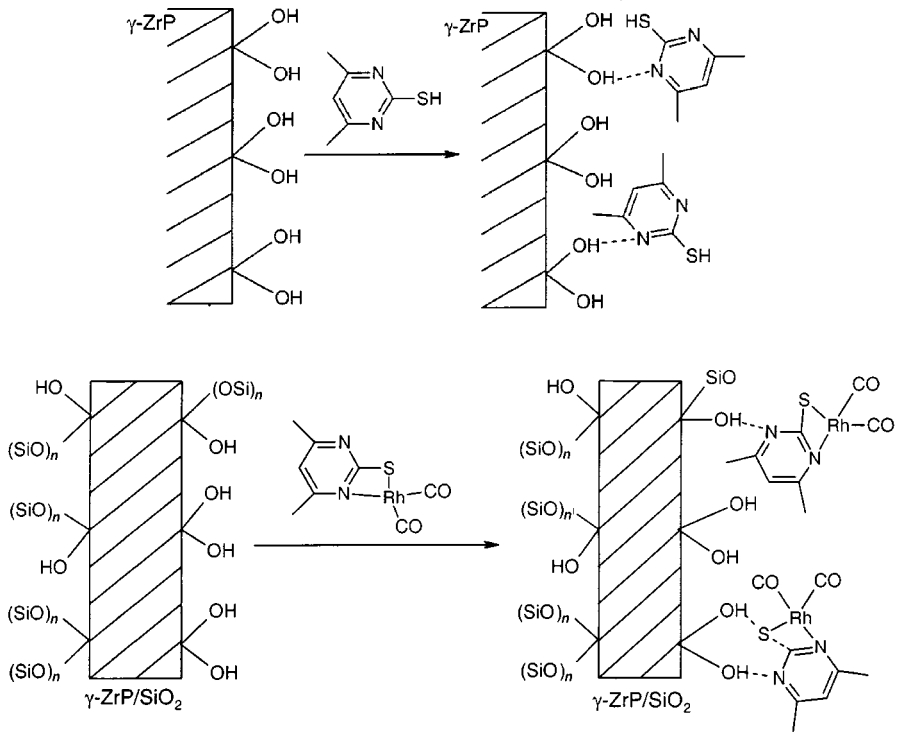

Scheme 2 (top) S1 synthesis proposal from γ-ZrP + HSpym. (bottom) RhS20-40 synthesis proposal from γ-ZrP-SiO_2 + RhSCO.

Table 1 Nomenclature and some physical data of the solids described

Solid	Comes from	Rh/wt%	$S_{BET}/m^2\ g^{-1}$	$V_{meso}/cm^3\ g^{-1}$
RhSCO	$[Rh(SN_2C_6H_7)(CO)_2]$	—	—	—
γ-ZrP	Crystalline support	—	6.5	—
20-ZPS	γ-ZrP(20 wt%) + SiO_2	—	488	0.367
40-ZPS	γ-ZrP(40 wt%) + SiO_2	—	493	0.342
S1	HSpym + γ-ZrP	0.00	10	0.000
S2	$[Rh(\mu\text{-}Cl)(CO)_2]_2$ + S1	7.15	11	0.000
S3	RhSCO + γ-ZrP	3.47	14	0.04
RhS20	RhSCO + 20-ZPS	0.64	378	0.312
RhS40	RhSCO + 40-ZPS	1.36	350	0.239

exchange process and from the catalytic cycles were determined by inductively coupled plasma atomic emission spectroscopy (ICP-AES), using a Perkin Elmer Optima 3300DV device. The solids were first treated with *aqua regia* at 363 K. Then, an aqueous solution of HF was added while maintaining the same temperature.

The specific area of the solid samples was calculated by the BET method applied to N_2 adsorption isotherms recorded on an ASAP 2010 apparatus at 77 K. Prior to nitrogen adsorption, samples were outgassed under vacuum at 383 K.

FTIR spectra were acquired on a Nicolet 510 spectrophotometer equipped with an MCT detector. Infrared spectra in the transmission mode were obtained on samples diluted in KBr (1 : 100) in the form of 12 mm diameter pressed discs, or as self-supported wafers.

Photoelectron spectra were recorded with a VG Escalab 200R electron spectrometer equipped with a Mg-Kα ($h\nu = 1253.6$ eV) X-ray source. Powdered samples were pressed into small stainless steel cylinders and outgassed at room temperature under a residual pressure of 10^{-6} mbar in the pretreatment chamber for 1 h. Then, the samples were transferred into the analysis chamber and analysis begun when the residual pressure reached 10^{-9} mbar. The Si 2p peak at a binding energy of 103.4 eV, or the Zr peak at a binding energy of 182.2 eV, was taken as an internal standard. Peak intensities were estimated by calculating the integral of each peak after subtraction of an S-shaped background and fitting the experimental peak to a combination of Lorentzian and Gaussian lines.

Catalytic activity measurements

The samples were transferred to a 100 mL stainless steel autoclave (Autoclave Engineers) fitted with inlet/outlet ports, a magnetic stirring device, a pressure measuring gauge and a heating system. Typically, *ca.* 25 mL of a mixture of 1-heptene (the precise amount to achieve a 1-heptene : Rh molar ratio of 353 : 1) in previously dried toluene, was used. The precise amount of Rh complex required for a concentration of 1.23×10^{-3} M was deposited in the autoclave vessel and outgassed at 383 K for 1 h. Then, the olefin–toluene mixture was injected while the pressure inside the reactor was set at 3 bar CO until the reaction temperature was reached (343 K). Then, a CO–H_2 gas mixture was admitted and pressure was increased up to 8 bar, achieving a CO : H_2 molar ratio of 1 : 1 while stirring at a rate of 750 rpm. Liquid samples were collected at regular time intervals. Conversion to the different products was determined by injection of the liquid sample into a gas chromatograph fitted with an HP Innowax column and a flame ionisation detector.

When the catalyst was used in consecutive hydroformylation reactions of 1-heptene, the reaction mixture obtained after the first cycle was separated by centrifugation. The solid catalyst was dried under vacuum, and used for the hydroformylation of a new cycle of 1-heptene, following the procedure described for the first cycle. The Rh : alkene molar ratio in each cycle was kept constant. The rhodium content of the catalyst was analysed before each hydroformylation cycle.

Results and discussion

Catalyst characterisation

Crystalline pathway. In order to carry out an accurate study of the interaction between the rhodium complex RhSCO and the SiO_2-modified γ-ZrP support, our first attempt was to introduce the ligand and the rhodium complex within the crystalline solid in a one- or two-step process. In the two-step procedure, solids S1 and S2 were obtained. The first step was the intercalation of the thiopyrimidine ligand (HSpym) in the crystalline γ-ZrP yielding solid S1. Solid S2 was obtained when complex $[Rh(\mu\text{-}Cl)(CO)_2]_2$ reacted with the intercalated ligand.

Chemical analysis of sample S1 revealed a S/Zr ratio of 0.5. This value corresponds to 25% exchange of the protons of the lamella with the ligand. The interlayer spacing in S1 was consistent with a good intercalation of the HSpym ligand in the interlayer region since the spacing increased from a value of $d = 1.22$ nm in γ-ZrP to $d = 1.54$ nm in the intercalation compound [Fig. 1(A)]. Although the interlayer distance of the precursor is expanded, its crystallinity is preserved. Once the ligand had been fixed,[24] the next step was to introduce the rhodium complex $[Rh(\mu\text{-}Cl)(CO)_2]_2$, whose ligands are easily exchangeable by the HSpym ligand and may yield a complex analogous to RhSCO. As the Rh/S ratio is 0.7 in S2, it is inferred that the rhodium thiolate complex RhSCO was formed in the first instance. Analysis of S2 shows that the Rh/Zr ratio is 0.31. The Rh loading achieved following this methodology is close to the maximum amount previously reported[25] and the crystallinity of the solid remained unaltered during the exchange process. The FTIR and XPS spectra will be discussed in later sections.

In the one-step procedure, the RhSCO complex was intercalated directly in γ-ZrP, giving solid S3. In this case, a dramatic loss of crystallinity was detected [see Fig. 1(A)] probably due to the large size of the rhodium thiolate complex.

These results reveal that HSpym behaves as an optimal enlarging agent to incorporate rhodium complexes into the crystalline support. The main drawback of this kind of solid support for catalyts is the lack of accessibility to the active sites. This accessibility has been improved successfully through their modification by adding high specific area solids. As can be seen below, a silica additive is particularly suitable for this purpose.

Amorphous solid pathway. According to the method described previously,[28] the modification of crystalline γ-ZrP provides solids with larger specific BET areas than that of the precursor. Unfortunately, these modified solids exhibit poor crystallinity. The X-ray diffraction patterns of the SiO_2-modified γ-ZrP (20-, 40-ZPS) samples showed only two peaks: one at $d = 3.90$ nm corresponding to the mesoporous structure of the support, and a second very broad one at

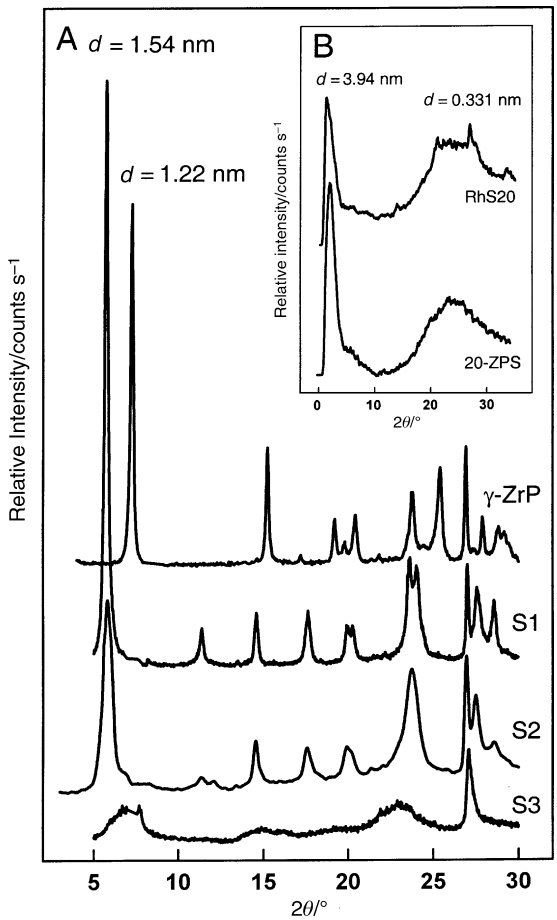

Fig. 1 Powder X-ray diffraction patterns of solids obtained through the crystalline pathway (A) and through the amorphous pathway (B) including support (20-ZPS) and fresh catalyst (RhS20).

$d = 0.418$ nm from the silica. Inset B in Fig. 1 shows an example of XRD patterns of a modified support containing 20% γ-ZrP (20-ZPS) and the corresponding catalyst (RhS20). The peak at $d = 0.331$ nm is ascribed to the γ-ZrP layer structure.

The specific area of the used RhS20 catalyst decreased from 378 to 46 $m^2\ g^{-1}$. However, it increased again close to the original value (*ca.* 310 $m^2\ g^{-1}$) after the oxo products were removed by toluene and acetone washing. The pore volume followed the same trend; used catalyst pore volume was 0.058 $cm^3\ g^{-1}$ but reached a value of 0.256 $cm^3\ g^{-1}$ after washing.

Likewise, the XRD patterns of RhS20 and RhS40 catalysts calcined at 1223 K show the appearance of the Rh_2O_3 phase and the absence of ZrP_2O_7 diffraction lines, which is consistent with the preservation of the mesoporous structure. The phosphorous/zirconium ratio is constant and equal to 2 throughout the overall process, also confirming the preservation of the zirconium phosphate content.

FTIR results. The interaction of the RhSCO complex with the SiO_2-modified ZrP substrate was revealed by looking at the background FTIR spectra of the samples. Both self-supported wafers and KBr-diluted pellets were examined. Although the spectra were quite similar in both cases, better resolution of the infrared bands was obtained for the KBr-diluted samples. Accordingly, the background spectra described here were recorded using the latter method. The infrared spectra of HSpym and several Rh-containing samples are shown in Fig. 2.

The bands centred between 1650–1450 cm^{-1} arise from vibrational modes characteristic of the thiopyrimidine ligand and may be indicative of how RhSCO interacts with the support. Unfortunately, these bands are the result of the contribution of two vibrational modes, CN stretching and NH deformation.[38] Therefore, it is extremely difficult to unequivocally assign them to a given bond. However, when the bands from RhS20 or RhS40 (Fig. 2, spectrum d) were compared with those of the free ligand (Fig. 2, spectrum a) and with the bands observed for S1 and S2 (Fig. 2, spectra b and c, respectively), and correlated with the bands observed previously[34] during study of the reactivity of the thiopyrimidine complexes, some conclusions regarding the nature of the interaction between the complex and the support can be derived. First, the band centred around 1630–1610 cm^{-1} was observed in all the spectra (Fig. 2, spectra a–d). In the thiopyrimidine precursor complexes, this band was associated with the presence of an N–H fragment.[34] When HSpym was intercalated in the crystalline γ-ZrP, the bands at 1629 and 1573 cm^{-1} shifted to 1631 and 1602 cm^{-1}, respectively (Fig. 2, spectrum b). The reduction of the peak-to-peak distance between these bands from 56 to 29 cm^{-1} might result from ligand constraints imposed by the interaction with the support. Bands centred at lower wavenumbers were red-shifted.

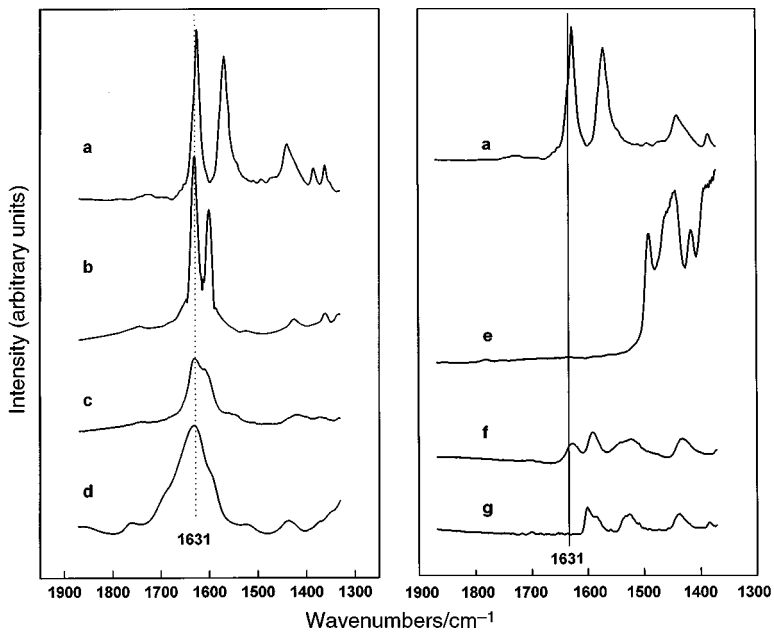

Fig. 2 FTIR spectra of selected samples. (a) HSpym, (b) S1, (c) S2, (d) RhS20, (e) $[Rh(\mu\text{-}Cl)(CO)_2]_2$, (f) $[Rh(Cl)HSpym(CO)_2]$, (g) RhSCO.

When $[Rh(\mu\text{-}Cl)(CO)_2]_2$ was introduced in solid S1, the band at 1631 cm^{-1} remained virtually unshifted, while the band at 1602 cm^{-1} moved to 1609 cm^{-1} (separation of 22 cm^{-1}) (Fig. 2, spectrum c). In the ν_{CO} region spectrum of solid S2 a broad band was observed. After deconvolution, two peaks centred at 2070 and 2002 cm^{-1} were obtained. The FTIR ν_{CO} peaks in complex $[Rh(Cl)(HSpym)(CO)_2]$ (Scheme 1) are centred at 2075 and 2007 cm^{-1}. This feature allows us to propose that the $[Rh(\mu\text{-}Cl)(CO)_2]_2$ complex reacts with solid S1 to give Rh species akin to $[Rh(Cl)(HSpym)(CO)_2]$. For the RhSCO complex anchored to γ-ZrP/SiO_2, the spectrum exhibits a very intense and broad band centred at 1631 cm^{-1} (Fig. 2, spectrum d) with several shoulders. In accordance with the rest of the spectra of the series, this band is assigned to an N–H fragment. Since this band was originally absent in the spectrum of the RhSCO complex[34] (Fig. 2, spectrum g) but was present in the protonated form of this complex (Fig. 2, spectrum f) it should have been formed during the anchoring of the complex. This is indicative of the nature of the N–H interaction between RhSCO and the amorphous support.

Study of the region between 1400–1300 cm^{-1} was also of great interest since this gives information about the $\nu_{C=N} + \nu_{C=S} + \delta_{C-H}$ modes.[39] In the free ligand, bands at 1440 cm^{-1} and several bands between 1386 and 1365 cm^{-1} were observed. The band at 1440 cm^{-1} was present in the rest of the spectra, while the bands around 1320–1380 cm^{-1} were also observed in spectra b and c, but not in the spectrum of the amorphous catalyst. The intensity of these bands was lowered after the anchoring process. This feature may be tentatively assigned to the non-chelating nature of the ligand to the metal, in spite of their typical behaviour.[34] Below 1300 cm^{-1}, the bands of the support overlap with the bands of the complex.

XPS results. Surface analysis by photoelectron spectroscopy (XPS) of selected samples was performed (Table 2). The N 1s core level spectra of the HSpym exchanged in the crystalline γ-ZrP support (sample S1) showed 2 peaks at 398.2 and 400.2 eV, assigned to a non-protonated and a protonated N atom of the ligand, respectively. From these spectra, the N/S atomic ratio was 2, in accordance with the stoichiometry of the thiopyrimidine ligand. When the RhSCO complex was tethered on the amorphous support (samples RhS40 and RhS20) this ratio increased up to a value of 4 or higher. The binding energies of the N 1s core level spectra of RhS20 showed peaks at 399.7 and 401.7 eV, which can be ascribed to NH and NH^+ forms of the N atoms in the complex. A similar spectrum has already been observed for the RhS40 counterpart. The N/Rh ratio was close to the stoichiometric value of 2 for both RhS40 and RhS20 samples. Apparently, the sulfur-containing species have been displaced from the outer surface of the catalyst since S was not detected by XPS, although it was detected by means of atomic emission spectroscopy, affording an S/Rh ratio between 0.7 and 0.8 for all the samples. The binding energy spectrum of the Rh $3d_{5/2}$ core level of the RhS40 catalyst displayed peaks centred at 307.2, 308.5 and 309.9 eV, assigned to Rh^0, Rh^+ and Rh^{3+} species. Rh^0 species may arise from the reductive agglomeration of Rh^+ species in the presence of CO, while the Rh^{3+} species would presumably be formed through oxidation of RhSCO during the anchoring step to the solid, since the reaction was conducted under ambient atmosphere. Solid RhS20 displayed two components in the Rh $3d_{5/2}$ peak, one at 307.8 due to Rh^0, and another at 309.0 eV, associated with Rh^+ species, shown in Fig. 3(A). When RhS20 was used as a catalyst during 5 consecutive cycles, Rh^{3+} species were also detected by XPS [Fig. 3(B)]. However, the fraction of Rh^+ in the solid surface remained stable (the activity of the catalyst was also maintained through several cycles of the reaction). The depletion of the Rh/Zr atomic ratio from 0.15 to 0.02 after re-using the catalyst over 5 cycles in the hydroformylation reaction indicates that metal leaching from the outer surface of the solid particles has occurred during the operation (Table 2). This fact was even more evident in the RhS40 catalyst, where the S 2p peak of the fresh sample was detected in the photoelectron spectrum, but that for the used catalyst virtually disappeared.

Catalytic activity results for heptene hydroformylation

The hydroformylation of 1-heptene was performed using rhodium thiolate complexes anchored to γ-ZrP, 20-ZPS and 40-ZPS substrates, corresponding to catalysts S3, RhS20 and RhS40, respectively. When the crystalline sample S3 was used as a catalyst in the hydroformylation of 1-heptene, at 343 K, 8 bar total pressure ($H_2/CO = 1$) and $PPh_3/Rh = 3$ the reaction products detected were mainly aldehydes; chemoselectivity was 98% and the terminal-to-internal aldehyde ratio (n/i) was 4.8. However, the reaction rate was very low, with values of 1-heptene conversion of *ca.* 18% being obtained after 72 h. The behaviour of the amorphous catalyst was monitored for several consecutive reaction cycles. The effect of the support nature (RhS20 *vs.* RhS40) and the addition of external triphenylphosphine were also studied.

When the reaction was conducted with the amorphous catalysts RhS20 and RhS40, after complete reaction, the liquid phase mainly consisted of aldehydes, both octanal (A1) and 2-methylheptanal (A2), and some heptene isomers. Neither hydrogenation nor higher oxo products were detected. When RhS20 was used as catalyst (at 343 K and 8 bar total pressure $H_2/CO = 1$), the addition of external PPh_3 seemed to be necessary for aldehydes to be obtained. In the absence of triphenylphosphine, the reaction mainly yielded heptene isomers,

Table 2 XPS binding energies (eV) of core electrons and surface atomic ratios of selected solids

Solid	S1	S2	RhS20	RhS40	RhS20 (used)
Zr $3d_{5/2}$	182.3	182	183.4	183.1	183.4
P 2p	132.9	133	134.4	133.5	133.9
Si 2p	—	—	103.4	103.4	103.4
Rh $3d_{5/2}$	—	308	307.8(56)	307.2(17)	307.4(36)
			309.0(44)	308.5(45)	308.9(44)
				309.9(37)	309.9(20)
N 1s	398.2(53)	399	399.7(61)	399.5(94)	390.7(16)
	400.2(47)		401.7(39)	401.6(6)	400.4(47)
					401.7(36)
S 2p	162.1	162	—	162.8	—
P/Zr	2.08	2.5	1.93	1.82	2.23
Si/Zr	—	13.9	13.8	16.4	12
Rh/Zr	—	0.06	0.15	0.85	0.02
N/Zr	0.5	0.3	—	1.59	0.02
S/Zr	0.23	—	—	0.38	—

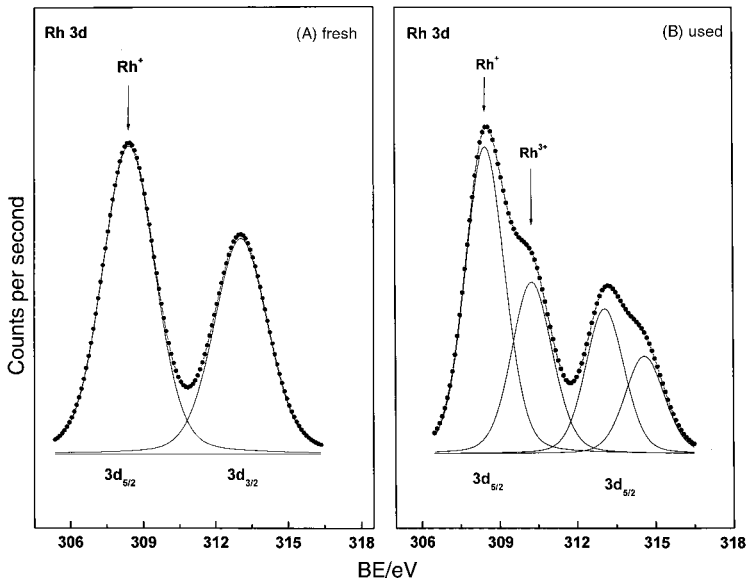

Fig. 3 Rh $3d_{5/2}$ core level spectra of the catalyst RhS20: (A) fresh and (B) after use in the hydroformylation of 1-heptene for 5 consecutive reaction cycles.

no oxo products being detected. Such an effect is ascribed not only to the absence of active hydroformylation centres, but also to the acidity nature of the support. The acid centres, mainly the Brönsted acidity on hydroxyl groups present on the support surface, are responsible for the isomerisation reaction. It should be noted that a pH value close to 5 was measured for the solid phase collected at the end of the reaction and dispersed in water.

Table 3 shows some selected data obtained for the hydroformylation reaction of 1-heptene performed with RhS20 at 343 K, total pressure 8 bar ($H_2/CO = 1$), $PPh_3/Rh = 3$ (molar ratio) and 1-heptene/Rh = 353 (molar ratio) in every cycle for 5 consecutive reaction cycles. The chemoselectivity for aldehyde and the regioselectivity for linear aldehyde values were similar in all reaction cycles. Activity profiles, expressed as 1-heptene conversion as a function of time, are shown in Fig. 4. These curves follow typical S-shape profiles and were similar for all the reaction cycles. The total turnover number was 1150 mol aldehyde per mol rhodium. From the FTIR spectra of the liquid samples no carbonyl assigned bands were detected beyond the second cycle. In order to determine whether rhodium was leached from the catalyst, the solid was analysed by atomic emission spectroscopy. The data obtained are shown in Table 3. The loss of rhodium was the highest during the first cycle. This fact was expected since the supported catalyst was not Soxhlet-washed after preparation. A major contribution to this rhodium loss during reaction was ascribed to rhodium species weakly adsorbed onto the catalyst. As expected, the liquid phase obtained from the first cycle was active in a subsequent hydroformylation reaction of 1-heptene, performed under homogeneous conditions. This is consistent with the presence of the Rh complex in solution. In consecutive cycles, the amount of rhodium leached from the catalyst during the reaction decreased markedly.

Table 3 Selected data obtained for the hydroformylation of 1-heptene in toluene during 5 consecutive cycles with catalyst RhS20[a]

Cycle	X[b](%)	Time/h	Chem[c](%)	n/i[d]	TOF[e]	Rh[f]/wt%
1	97	30.7	99	4.5	13.5	0.6
2	97	22.3	99	4.4	28.4	0.4
3	99	25.6	99	4.3	35.4	0.35
4	99	25.7	99	4.8	39.6	—
5	98	25.9	97	3.8	46.2	0.2[g]

[a] Reaction conditions: $P = 8$ bar ($H_2/CO = 1$), $T = 343$ K, for every cycle 1-heptene/Rh molar ratio = 353; PPh_3/Rh molar ratio = 3. [b] 1-Heptene conversion. [c] Chemoselectivity (total aldehydes/total products). [d] Linear aldehydes/branched aldehydes ratio. [e] Maximum TOF at a given time defined as mol aldehyde per mol rhodium per hour. [f] Rh content of the catalyst at the beginning of the cycle. [g] Rh content of the catalyst at the end of the cycle.

When the behaviour of complex RhSCO was monitored in homogeneous media,[40] under similar conditions as used with solid RhS20 and RhS40, [*i.e.*, substrate 1-heptene, temperature 343 K, total pressure 8 bar ($H_2/CO = 1$), $PPh_3/Rh = 3$ and 1-heptene/Rh = 353] several differences were observed. First, the reaction proceeds faster in the "heterogeneous phase", than in the homogeneous one (TOF = 30 h^{-1} in the homogeneous phase). Furthermore, the n/i ratio was 2.9 in the homogeneous phase, while it was 4.4 and 3.9 for solids RhS20 and RhS40, respectively.

After each reaction cycle, the solid catalyst was separated under air by centrifugation. Before and after this process, the BET area of the solid was measured. It was found that the

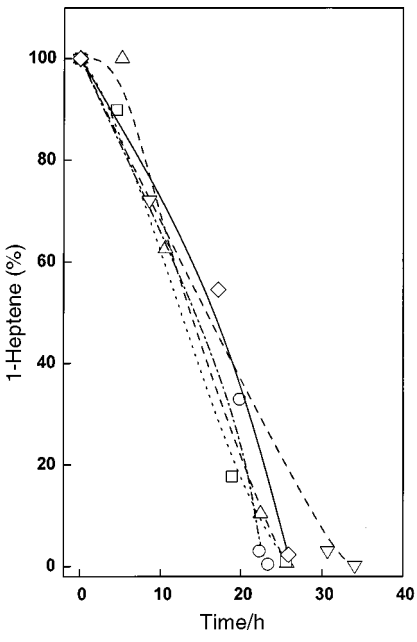

Fig. 4 1-Heptene conversion profiles obtained for catalyst RhS20 during 5 consecutive reaction cycles: 1st (▽), 2nd (○), 3rd (□), 4th (△) and 5th (◇) cycles.

BET area of the catalyst diminished strongly once it had been used, even after the separation process. Since this decrease must be due to the reaction products being strongly retained within the pores of the solid, the used catalyst was washed first with toluene, then with acetone and then separated again by centrifugation. After this cleaning process the BET area of the catalyst was almost restored to the value of the fresh catalyst. The loss in BET area of the used catalyst is due to the presence of aldehydes and toluene strongly adsorbed within the catalyst pore network. GC analysis of the acetone employed in the washing process of the used catalyst revealed the presence of toluene and aldehydes, thus confirming the working hypothesis of pore plugging by the reaction products and solvent. Under reaction conditions, these species may presumably desorb rapidly in agreement with the equilibrium between the solid and liquid phases in the reactor. Thus, the active sites of the catalyst do not appear to be blocked during the reaction. It is known that Rh catalysts may be readily oxidised in air,[41] but the presence of these absorbed species may hinder the diffusion of O_2 towards the metal centres, thus preventing catalyst deactivation when it is exposed to air during the separation process, at least in the early stages of the process. Some oxidation at the outer surface of the catalyst particles is unavoidable, as already detected by XPS.

When the reaction was conducted with catalyst RhS40 at 343 K, total pressure 8 bar ($H_2/CO = 1$), $PPh_3/Rh = 3$ and 1-heptene/Rh = 353, aldehydes A1 and A2 were the main products detected. The chemoselectivity to aldehydes was similar to that achieved with the RhS20 catalyst. However, the linear-to-branched aldehyde ratio decreased slightly. The reaction rate was higher than that observed with catalyst RhS20. The results obtained after the second reaction cycle had been completed are shown in Table 4. The increase in the reaction rate of catalyst RhS40 with respect to its RhS20 counterpart can be understood by looking at the Rh/Zr atom ratios derived from XPS measurements (Table 2). The increase in the Rh/Zr ratio by a factor of *ca.* 6 in catalyst RhS40 indicates that Rh is highly exposed on the surface and surface region of the delaminated Zr phosphate phase. Thus, a higher density of Rh complex units is available in this sample for the reaction, and these are responsible for the high TOF value observed (168 h^{-1}).

The effect of the amount of added PPh_3 ($PPh_3/Rh = 3$ and 30) was monitored for catalysts RhS20 and RhS40. As a general rule, the presence of a large excess of PPh_3 makes the reaction more selective towards the linear aldehyde (A1). However, the reaction rate follows an opposite trend, while for catalyst RhS40 the reaction becomes slower, an excess of PPh_3 accelerates the reaction rate for catalyst RhS20. Some selected data illustrating this behaviour are depicted in Table 4.

Similarly, Fig. 5 shows the 1-heptene consumption profiles obtained, using catalysts RhS20 and RhS40 as a function of the amount of PPh_3 added. The curves correspond to the second cycle of the reaction, except in the case of catalyst RhS40 ($PPh_3/Rh = 30$), corresponding to the third cycle of the reaction.

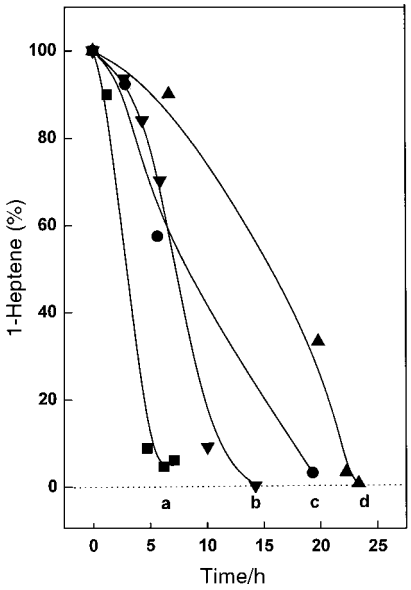

Fig. 5 Effect of the amount of PPh_3 and support acidity in the hydroformylation of 1-heptene: (■, a) RhS40, $PPh_3/Rh = 3$; (▼, b) RhS20, $PPh_3/Rh = 30$; (●, c) RhS20, $PPh_3/Rh = 3$; (▲, d) RhS40, $PPh_3/Rh = 30$.

As stated above, some rhodium leached into the liquid phase during the hydroformylation process. The amount of rhodium loss was determined by plasma analysis of the remaining solid. Losses were high in the first cycle of the reaction for all the catalysts studied. Preferential removal of rhodium from the outer catalyst surface takes place, as shown by the XPS Rh/Zr ratio, which decreases drastically as compared to the Rh/Zr ratio determined by chemical analysis. This indicates that the hydroformylation reaction is mainly confined to the interlayer space of the zirconium phosphate sheets where Rh is still present, in agreement with chemical analysis.

RhS20 and RhS40 are active in the hydroformylation of 1-heptene under mild reaction conditions (*i.e.*, 8 bar total pressure and 343 K). More severe reaction conditions such as 30,[30] 40,[22] or 50 bar total pressure[42] or a pressure range of 30–90 bar[43] have been used for other Rh heterogeneised catalysts. The only catalysts active under milder conditions have been reported by Gao and Angelici.[20,31] However, at similar PPh_3/Rh molar ratios, RhS20 and RhS40 were more active than the catalyst in ref. 20 (which displayed a conversion of *ca.* 30% *vs. ca.* 95%) and more selective towards aldehydes than the catalysts reported in ref. 31, which yields 15% of alkene isomers; furthermore the n/i ratio (*ca.* 3.4) was higher using catalysts RhS20/40 (*ca.* 4.3).

Conclusions

The reaction of $[Rh(\mu\text{-}Cl)(CO)_2]_2$ complex with enlarged γ-ZrP-HSpym affords a highly crystalline and almost completely exchanged γ-ZrP-RhSCO derivative. This solid is suit-

Table 4 Selected data obtained for the hydroformylation of 1-heptene in toluene with RhS20 and RhS40 catalysts during the 2nd reaction cycle[a]

Solid	X[b](%)	Time/h	Chem[c](%)	n/i[d]	TOF[e]	PPh_3[f]	Rh[g]
RhS20	97	22.3	99	4.4	28.4	3	0.83
RhS40	96	7.1	99	3.9	167.9	3	0.97
RhS20	97	19.3	98	5.4	38.1	30	0.84
RhS40[h]	93	25.2	100	5.5	6.8	30	0.96

[a] Reaction conditions: $P = 8$ bar ($H_2/CO = 1$), $T = 343$ K, for every cycle 1-heptene/Rh molar ratio = 353. [b] 1-Heptene conversion. [c] Total aldehyde/total products ratio. [d] Linear aldehyde/branched aldehyde ratio. [e] Maximum turnover frequency defined as mol aldehyde per mol rhodium per hour. [f] PPh_3/Rh molar ratio. [g] Rh_f/Rh_i ratio (Rh_i and Rh_f are the Rh amounts at the beginning and end of the cycle, respectively). [h] Data obtained for the 3rd reaction cycle.

able for a structural study to be carried out. The anchoring of RhSCO complex onto zirconium acid phosphates is achieved *via* hydrogen bonds forming NH groups. This interaction affords catalyst precursors that are stable during the hydroformylation of 1-heptene, and although they lose part of the Rh during the reaction, it seems that the thiolate complex renders stable Rh reservoirs. The Rh loss is moderate, and permits the reuse of the catalyst for at least 5 consecutive cycles with no decrease in activity. The heterogeneous hydroformylation performed with the rhodium thiolate supported catalyst was faster and more selective than the process performed with the rhodium complex in homogeneous media. The Rh^+ species remain stable during the catalytic reaction, while Rh^0 was partially oxidised to Rh^{3+}. During the process, the activity of the catalyst was not modified. The S release from the catalyst, which maintains its activity, reveals that thiolate species are not intermediates in the hydroformylation reaction.

Acknowledgements

This research was partly supported by the Interministerial Commission of Science and Technology (CICYT), Spain, under project QUI98-0784. S. M. M. expresses her appreciation to the Ministry of Science and Technology for a contract and S. R. thanks the FEDER programme (Project 1FD97-0176) for a fellowship.

References

1 M. Beller, B. Cornils, C. D. Frohning and C. W. Kohlpaintner, *J. Mol. Catal. A: Chem.*, 1995, **104**, 17 and references therein.
2 D. Neibecker and R. Réau, *J. Mol. Catal.*, 1989, **53**, 219.
3 I. Amer and H. Alper, *J. Am. Chem. Soc.*, 1990, **112**, 3674.
4 S. Gladiali, L. Pinna, C. G. Arena, E. Rotondo and F. Faraone, *J. Mol. Catal.*, 1991, **66**, 183.
5 W. Chen, Y. Xu and S. Liao, *J. Mol. Catal.*, 1994, **88**, 277.
6 C. D. Frohning and C. W. Kohlpaintner, in *Applied Homogeneous Catalysis with Organometallic Compounds*, ed. B. Cornils and W. A. Hermann, VCH, Weinheim, 1996, p. 29.
7 C. U. Pittman, in *Polymer Supported Catalysts*, ed. G. Wilkinson, F. G. A. Stone and E. W. Abel, Pergamon Press, Elmsford, NY, 1983, p. 553.
8 S. J. Shuttleworth, S. M. Allin and P. K. Sharma, *Synthesis*, 1997, 1217.
9 J. W. J. Knapen, A. W. van der Made, J. C. de Wilde, P. W. N. M. van Leeuwen, P. Wijkens, D. M. Grove and G. Van Koten, *Nature* (*London*), 1994, **372**, 659.
10 L. Pu, *Chem. Rev.*, 1998, **98**, 2405.
11 T. Sawaki and Y. Aoyama, *J. Am. Chem. Soc.*, 1999, **121**, 4793.
12 N. Herron, *CHEMTECH*, 1989, **19**, 542.
13 S. Kobayashi, M. Endo and S. Nagayama, *J. Am. Chem. Soc.*, 1999, **121**, 11229.
14 J. Blum, D. Avnir and H. Schumann, *CHEMTECH*, 1999, **29**, 32.
15 E. Davis, *CHEMTECH*, 1992, **22**, 498.
16 L. P. Barthel-Rosa and J. Gladysz, *Coord. Chem. Rev.*, 1999, **190**, 587.
17 P. Wentworth and K. D. Janda, *Chem. Commun.*, 1999, 1917.
18 B. Pugin, *J. Mol. Catal. A: Chem.*, 1996, **107**, 273.
19 J. M. Basset and J. P. Niccolai, in *Applied Homogeneous Catalysis with Organometallic Compounds*, ed. B. Cornils and W. A. Hermann, VCH, Weinheim, 1996, p. 624.
20 H. Gao and R. J. Angelici, *J. Mol. Catal. A: Chem.*, 1999, **145**, 83.
21 T. J. Marks, *Acc. Chem. Res.*, 1992, **25**, 57.
22 S. Bischoff, A. Köckritz and M. Kant, *Top. Catal.*, 2000, **13**, 327.
23 P. Gianncoccaro, E. De Giglio, M. Gargano, M. Aresta and C. Ferragina, *J. Mol. Catal. A: Chem.*, 2000, **157**, 131.
24 P. Giannoccaro, A. La Ginestra, M. A. Massucci, C. Ferragina and G. Mattogno, *J. Mol. Catal. A: Chem.*, 1996, **111**, 135.
25 C. Ferragina, P. Cafarelli and R. Di Rocco, *Mater. Res. Bull.*, 1998, **33**, 305.
26 G. Alberti, U. Costantino, S. Murcia-Mascarós and R. Vivani, *Supramol. Chem.*, 1995, **6**, 29.
27 G. Alberti, D. C. Dionigi, E. Giontella, S. Murcia-Mascarós and R. Vivani, *J. Colloid Interface Sci.*, 1998, **188**, 27.
28 G. Alberti, S. Cavalaglio, F. Marmottini, K. Mabusek, J. Megyeri and L. Szirtes, *Appl. Catal.*, 2001, **218**, 219.
29 M. Eisen, J. Blum and H. Schumann, *J. Mol. Catal.*, 1985, **31**, 317.
30 J. L. G. Fierro, M.-D. Merchán, S. Rojas and P. Terreros, *J. Mol. Catal. A: Chem.*, 2001, **166**, 255.
31 H. G. Gao and R. J. Angelici, *Organometallics*, 1998, **17**, 3063.
32 P. Kalck and F. S. Spirau, *New J. Chem.*, 1989, **13**, 515.
33 G. Alberti, E. Giontella and S. Murcia-Mascarós, *Inorg. Chem.*, 1998, **37**, 4672.
34 S. Rojas, J. L. G. Fierro, R. Fandos, A. Rodriguez and P. Terreros, *J. Chem. Soc., Dalton Trans.*, 2001, 2316.
35 G. Giordano and R. H. Carabtree, *Inorg. Synth.*, 1990, **28**, 89.
36 J. A. McCleverty and G. Wilkinson, *Inorg. Synth.*, 1990, **28**, 85.
37 L. Walz and T. Scheer, *Acta. Crystallogr., Sect. C*, 1991, **47**, 640.
38 C. N. R. Rao and R. Venkataraghavan, *Spectrochim. Acta*, 1962, **18**, 541 and references therein.
39 B. Singh, M. M. P. Rukhaiyar and R. J. Sinha, *J. Inorg. Nucl. Chem.*, 1977, **39**, 29.
40 S. Rojas, PhD Thesis, UAM, Madrid, 1999.
41 M. Krom, R. G. E. Coumans, J. M. M. Smits and A. W. Gal, *Angew. Chem., Int. Ed.*, 2001, **40**, 2106.
42 J. A. Díaz-Auñón, M. C. Román-Martínez and C. Salinas-Martínez de Lecea, *J. Mol. Catal. A: Chem.*, 2001, **170**, 81.
43 N. Yoneda, Y. Nakagawa and T. Mimami, *Catal. Today*, 1997, **36**, 357.